

Abundance and Systematics of Nuclear Superdeformed States; Relation to the Pseudospin and Pseudo-SU(3) Symmetries

J. Dudek

Center de Recherches Nucléaires et Université Louis Pasteur, F-67037 Strasbourg Cedex, France

W. Nazarewicz

Institute of Physics, Technical University, PL-00-662 Warsaw, Poland

Z. Szymanski

Centre de Recherches Nucléaires, F-67037 Strasbourg Cedex, France, and Institute of Theoretical Physics, Warsaw University, PL-00-681 Warsaw, Poland

and

G. A. Leander

Oak Ridge Associated Universities, Oak Ridge, Tennessee 37830

(Received 31 December 1986)

Results of a multidimensional (β_2 , γ , β_4 , ω , Z , and N) search for nuclear superdeformed configurations are presented. Calculations based on a realistic deformed average field give a relatively strong dependence of the "super" elongation on the particle number. This dependence is shown to be a cyclic function of the particle number. It originates from the pseudospin and pseudo-SU(3) symmetries which are obeyed approximately in a realistic average field.

PACS numbers: 21.10.Gv, 21.60.Fw

Nuclear states are commonly called superdeformed if the spatial distribution of nuclear matter is strongly elongated (cf. related harmonic-oscillator structures¹). In view of the recent discovery² of a rotational band built on the superdeformed states in ¹⁵²Dy and extending up to $I_{\max}=60$, and another one³ in ¹³²Ce extending up to $I_{\max}\approx 52$, the prospect of detailed studies of the structure, population, and decay of such bands opens up. The need for their uniform and possibly general classification and abundance scheme becomes apparent.

We base our analysis on the deformed Woods-Saxon average field⁴ and the Strutinsky⁵ approach in the versions of Andersson *et al.*,⁶ Bengtsson and Ragnarsson,⁶ and Dudek and Nazarewicz.⁶ We consider the deformation space spanned by the quadrupole (β_2, γ) and the hexadecapole (β_4) degrees of freedom. Nuclear rotation is accounted for by the introduction of the rotational frequency ω in the usual one-dimensional cranking approach (cf., e.g., Ref. 6).

Let us summarize the results of our multistep procedure. First the single-particle levels were tabulated versus β_2, γ and β_4 at $\omega=0$. The strongest shell-structure effects resulted for axial symmetry, i.e., for $\gamma\approx 0^\circ$, many of them weakly dependent on β_4 in a relatively large β_4 range. Therefore the global features of the Woods-Saxon single-particle spectra will be discussed as functions of β_2 and displayed along one single trajectory in (β_2, β_4) space representative of many nuclei. Systematic detailed calculations showed that the steepest-descent lines in the total-energy surfaces lie

close to this trajectory for most of the nuclei considered here. The neutron single-particle levels are displayed along such a trajectory in Fig. 1. The areas of increased level density are shaded. The spectrum exhibits several stripes of low level density. We refer to the stripes as *chains* of deformed shell closures. Analogous features hold for the proton spectrum and are strikingly similar to those found¹¹ in the Nilsson model.

To suggest a possible origin of the regularities demonstrated in Fig. 1, we introduce the spectrum of the pseudo-oscillator. It is obtained from that of the harmonic oscillator by ignoring all the states which, after introduction of spin-orbit interaction, will give rise to the $l=I_{\max}=N$ (intruder) orbitals. We denumerate the remaining levels using the pseudo-oscillator quantum numbers $\tilde{N}=N-1$, $\tilde{n}_z=n_z$, each level carrying $(2s+1)(\tilde{N}-\tilde{n}_z+1)$ degeneracy (spin $s=\frac{1}{2}$). A Hamiltonian generating such a spectrum is said to obey the pseudo-SU(3) symmetry.^{8,12} An example of the resulting single-particle level pattern is given in Fig. 2, where the appropriately modeled intruder levels have also been placed. Although the intruder levels do not belong to the pseudo-oscillator pattern, their presence is necessary to reproduce correctly the realistic occupation scheme.

Striking similarities between the spectra of Figs. 1 and 2 may be viewed as a manifestation of the *approximate* pseudo-SU(3) symmetry of the deformed Woods-Saxon potential (for the Nilsson potential cf. Ref. 11).

Let us also emphasize the presence of yet another approximate symmetry (called pseudospin^{9,10}) in the axial-

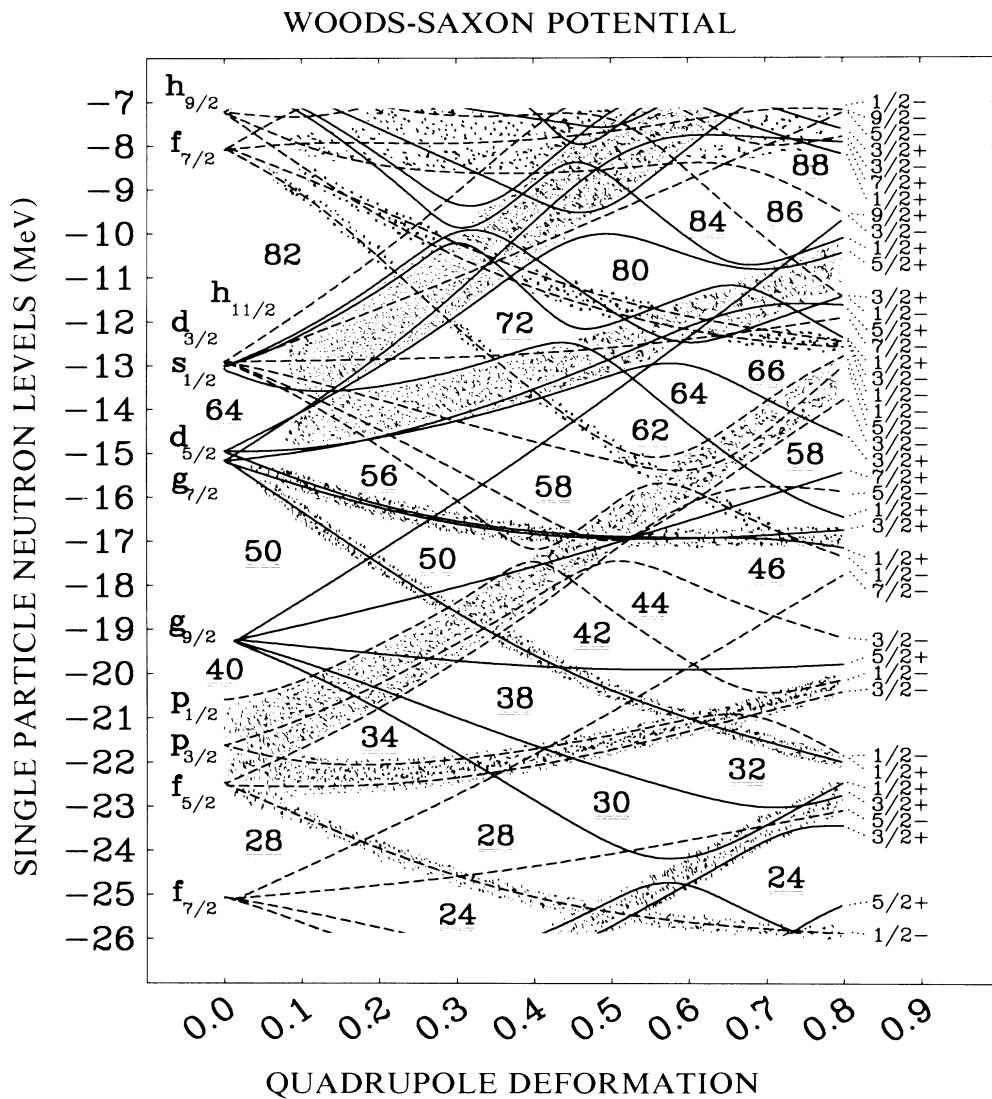


FIG. 1. Neutron single-particle spectra calculated along $(\beta_2, \beta_4, \gamma=0^\circ)$ trajectory which minimizes the liquid-drop-model energy of Ref. 7 at spin $I=60$. Groups of single-particle levels analogous to those in the pseudo-oscillator scheme of Fig. 2 are shaded. The displayed spectrum corresponds to nucleus $Z_0=66, N_0=86$ but is representative for a broad range of particle numbers. Relation to the pseudo-SU(3) symmetry is suggested via analogies to results in Fig. 2; cf. also Refs. 8-10.

ly symmetric Woods-Saxon field. Its manifestation lies in an approximate degeneracy between the deformed field levels $[\tilde{N}\tilde{n}_z\tilde{\Lambda}]_{\Omega=\tilde{\Lambda}+1/2}$ and $[\tilde{N}\tilde{n}_z\tilde{\Lambda}]_{\Omega=\tilde{\Lambda}-1/2}$ (intruder states excluded). These levels originate from the $l_j=l+1/2$ and $(l+2)_{j'=j+1}$ spherical orbitals, cf. Fig. 1; $l \equiv l+1$ and $\tilde{\Lambda}$ denotes projection of \tilde{l} . It has been shown^{10,12} that such a symmetry implies an approximate conservation of the total projections $\sum \tilde{\Lambda}(i)$ and $\sum \tilde{s}_z(i)$ separately ($\Omega = \tilde{\Lambda} + \tilde{s}_z$), thus providing an additional classification of the multiparticle wave functions, important especially for light and very heavy nuclei where superdeformation appears *already at very low spin*.

One of the very successful nuclear effective interac-

tions, the surface δ interaction, is known to obey the pseudo-SU(3) symmetry; cf., e.g., Ref. 8. It seems particularly attractive to interpret the analogies between the results in Figs. 1 and 2 in terms of an approximate symmetry of the two-body interactions satisfied as well by the realistic average field.

It is *a priori* not obvious that the gaps present in the spectra of Fig. 1 are sufficiently strong to produce local minima in the total-energy surfaces at *high spins*. To check this we applied the Strutinsky approximation in the version of Ref. 6, cf. results in Fig. 3.

The local minima corresponding to the strongly elongated (superdeformed) configurations of nuclei with

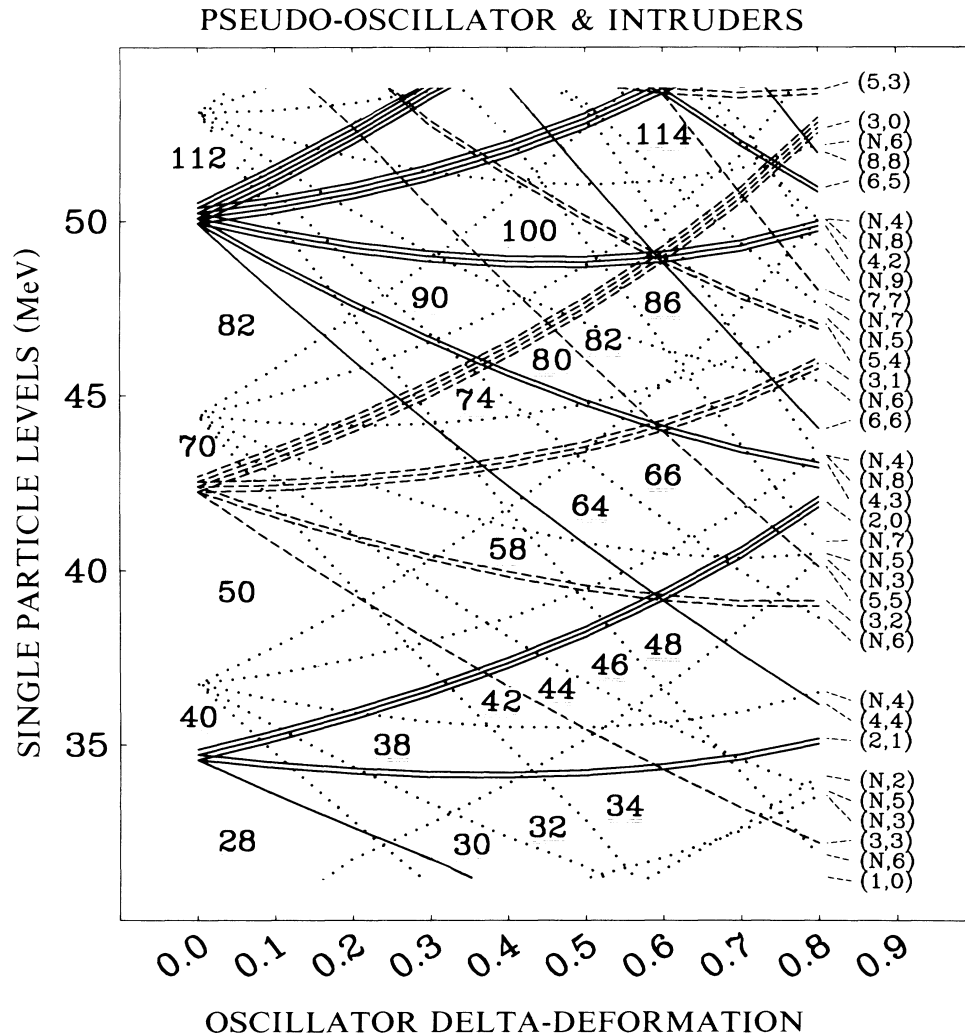


FIG. 2. Pseudo-oscillator-plus-intruder model spectrum constructed on the basis of the oscillator spectrum as follows. Oscillator orbitals which after introducing the $\mathbf{l} \cdot \mathbf{s}$ coupling give rise to the intruder multiplets are removed. The remaining scheme is called "pseudo-oscillator" and is related to the so-called pseudo-SU(3) symmetry (Refs. 8-10). The pseudo-oscillator labels in terms of $(\bar{N} = N - 1, \bar{n}_z = n_z)$ are given explicitly. The orbital $(\bar{N} - \bar{n}_z + 1)$ degeneracy is marked by the corresponding parallel lines. The intruder states [dotted lines labeled $(N, \text{actual } N \text{ value})$] stay outside the discussed symmetry and are modeled by shifting the corresponding oscillator shells. The positions of the intruder orbitals at spherical shapes imitate the positions of the corresponding Woods-Saxon intruders with respect to the main shells. Deformation defined with Eq. (5.11) of Ref. 1 satisfies, within linear approximation, $\delta \approx 0.95\beta_2$.

$N \approx 72$ to 74 are much smaller ($\beta_2 \approx 0.36$) as compared with those of $N = 80$ nuclei ($\beta_2 \approx 0.50$) and, further on, those of $N = 86$ ($\beta_2 \approx 0.60$ to 0.65). The results in Fig. 3 agree with experiment. Results for ^{132}Ce are compatible with the deformation $\beta_2^{\text{expt}} \approx 0.38$ (cf. Ref. 3), compared with $\beta_2^{\text{th}} \approx 0.36$; those for ^{152}Dy of Ref. 2 with $\beta_2^{\text{th}} \approx 0.65$. The present scheme is further supported by the results for ^{135}Nd ,¹³ and by the large prolate deformations observed in Sr isotopes^{14,15}; cf. the $Z = N = 38$ and $N = 42$ -58 gaps, Fig. 1.

The existence of nuclear rotation ($\omega \neq 0$) does not destroy strong openings in the ($\gamma \approx 0^\circ$) single-particle spectra over the large ω range; cf. also Ref. 11. This is because the normal-parity states are highly fragmented because of the large deformation and carry relatively small alignment. Rapid variations in the single-particle Routhian spectra are related to the strongly aligned intruder orbitals crossing the large openings at finite ω values. Consequently, at high spin the deformed closure chains may contain the particle values increased as com-

VARIATION in the SUPER-ELONGATION

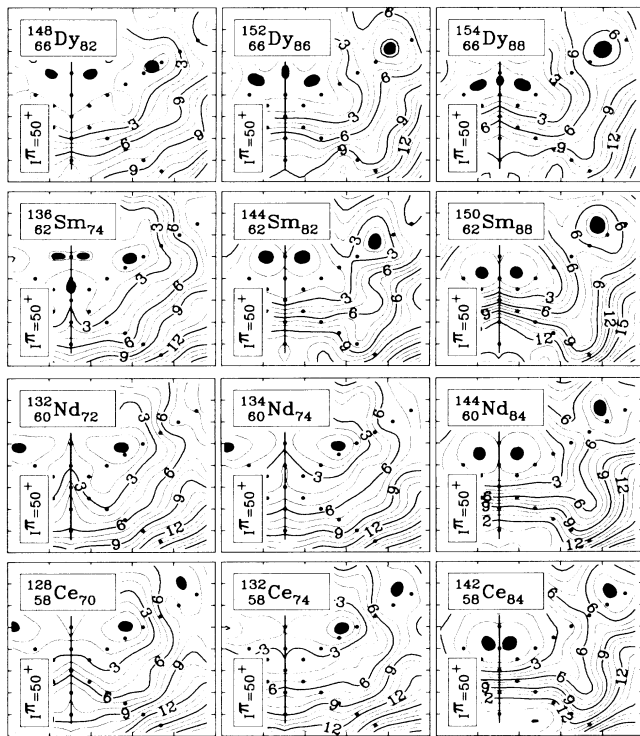


FIG. 3. Potential-energy surfaces in the (β_2, γ) plane at a fixed spin value $I=50$. The vertical axis in the field of the figure denotes $\gamma=60^\circ$ deformation ($\beta_2 > 0$, oblate shape, non-collective rotation) and $\gamma=-120^\circ$ ($\beta_2 < 0$, prolate shape, non-collective rotation). Rows of filled circles at $\Delta\beta_2=0.1$ intervals define the $\Delta\gamma=60^\circ$ sectors. The maps are given in polar coordinates and the horizontal axis is not the $\gamma=0^\circ$ axis. Note in particular that the cerium isotopes possess two elongated minima: the one at $\beta_2 \approx 0.36$ due to the neutron closure $N=72$ and a weaker one at $\beta_2 \approx 0.75$ due to the proton closure $Z=58$.

pared with those at $\omega=0$.

In summary, the realistic description of nuclear single-particle spectra manifests approximate pseudospin and pseudo-oscillator symmetries in the physical defor-

mation range. This feature is isospin independent.

Calculations show that the strongly elongated structures are attributed to *chains of particle numbers*. Within each chain deformations increase with the particle number. This coupling scheme explains a systematic abundance of strongly elongated shapes throughout the nuclear chart. From the existence of the chain structure it follows that there is no sharp distinction between the superdeformed and more familiar low-deformation regions. In fact, a broad range of stable nuclear deformation originates from the same pseudo-oscillator degeneracy pattern.

This work was supported in part by Polish Ministry of Science and Education under Contract No. CPBP 01.09 and by the U. S. Department of Energy under Contract No. DE-AC05-76OR003.

¹A. Bohr and B. R. Mottelson, *Nuclear Structure* (Benjamin, New York, 1975), Vol. 2.

²P. J. Twin *et al.*, Phys. Rev. Lett. **57**, 811 (1986); M. A. Bentley *et al.*, to be published.

³P. J. Nolan *et al.*, J. Phys. G **11**, L17 (1985); A. J. Kirvan *et al.*, Phys. Rev. Lett. **58**, 467 (1987).

⁴J. Dudek *et al.*, Phys. Phys. Rev. C **23**, 920 (1981); W. Nazarewicz *et al.*, Nucl. Phys. **A435**, 397 (1985).

⁵V. M. Strutinsky, Nucl. Phys. **A122**, 1 (1968).

⁶G. Andersson *et al.*, Nucl. Phys. **A268**, 205 (1976); T. Bengtsson and I. Ragnarsson, Nucl. Phys. **A436**, 14 (1985); J. Dudek and W. Nazarewicz, Phys. Rev. C **31**, 298 (1985).

⁷P. Möller and J. R. Nix, Nucl. Phys. **A361**, 117 (1981).

⁸R. D. Ratna Raju *et al.*, Nucl. Phys. **A202**, 433 (1973).

⁹A. Arima *et al.*, Phys. Lett. **30B**, 517 (1969).

¹⁰A. Bohr *et al.*, Phys. Scr. **26**, 267 (1982).

¹¹I. Ragnarsson *et al.*, Phys. Rep. **C45**, 1 (1978) (cf. Chap. 2), and Nucl. Phys. **A347**, 287 (1980); T. Bengtsson *et al.*, Phys. Scr. **24**, 200 (1981).

¹²K. T. Hecht and A. Adler, Nucl. Phys. **A137**, 129 (1969).

¹³E. M. Beck *et al.*, in Proceedings of the Workshop on Nuclear Structure, Berkeley, California, 1986, edited by M. A. Deleplanque (unpublished).

¹⁴C. J. Lister *et al.*, Phys. Rev. Lett. **49**, 308 (1982).

¹⁵R. E. Azuma *et al.*, Phys. Lett. **86B**, 5 (1979).